X-ray diffraction of bone at the interface with hydroxyapatite-coated versus uncoated metal implants

L. SAVARINO, S. STEA, D. GRANCHI, M. E. DONATI, M. CERVELLATI, A. MORONI*, G. PAGANETTO, A. PIZZOFERRATO
*Laboratory for Biocompatibility Research on Implant Materials and *Third Department of Orthopaedic Surgery, Istituti Ortopedici Rizzoli, Bologna, Italy*

The microstructural characteristics of the newly formed bone tissue at the interface with hydroxyapatite-coated and uncoated stainless steel pins used in an external fracture fixation system have been evaluated. The bone far from the interface was used as a control. Pins were transversally inserted into the diaphyses of sheep tibiae and were loaded in for six weeks. Three sheep received coated pins and two received uncoated pins. Crystallographic habit and mineralization of the implant-facing bone were evaluated. Moreover, lattice parameters of bone apatite were measured and hydroxyapatite (HA) coating degradation was investigated, by means of conventional and microbeam X-ray diffraction (XRD). In coated pins, six weeks after the implantation the newly formed bone tissue at the interface did not reach complete maturation, but the presence of the implant did not alter the apatite lattice structure; the lattice parameters did not show statistically significant variations with respect to those observed in the control bone. In uncoated pins, bone tissue rarely appeared totally mineralized and lattice parameters were significantly different with respect to those observed in the bone far from the implant. HA particles were observed spreading in the bone-facing coated pins; the XRD pattern of bone apatite surrounding HA particles was unmodified. It was concluded that HA coatings improved the bone remodelling process during pin fixation in comparison to uncoated pins and did not alter the crystallographic habit of apatite.

1. Introduction

Bone remodelling and the mineralization process at the interface are fundamental elements of good implant–bone fixation and, therefore, of the success of a prosthesis.

There is well documented proof in the literature that synthetic HA used as implants can bond to bone without bone resorption around it [1–4]; because of the presence of free calcium and phosphate ions at the surface, the implant is capable of interaction with the surrounding bone. In particular the use of HA is promising in that it has very similar chemical and crystallographic structures to the bone apatite, which effectively eliminates biocompatibility problems. For this reason, and because of the poor mechanical properties of the bulk HA ceramic, synthetic hydroxyapatite is proposed as a suitable coating material to achieve strong early fixation of uncemented prostheses [5].

The use of plasma-sprayed HA coating on implant surfaces has been shown to shorten the time needed to achieve adequate fixation strength and increase the maximum fixation strength that can be attained. HA coatings on metal implants enhance rapid bone formation and increase the amount of bone–implant apposition or bone ingrowth because of their osteoconductive properties, compared with uncoated implants [3, 6, 7]; moreover, they offer the potential advantages of limiting biological corrosion and ion release in periprosthetic tissues.

However, HA coatings obtained by plasma- spraying methods have several problems: it has been demonstrated that a significant decrease of the starting powder crystallinity caused by rapid cooling following the high temperature of the plasma flame results in the formation of amorphous calcium phosphate in the coating. The reduced crystallinity of HA can easily determine biodegradation or bioresorption of the coating in perimplant tissues and, therefore, alter bone remodelling.

Nevertheless, recently, coating application has been extended to pins used in external fracture fixation systems [7–9]. These orthopaedic devices are applied in fracture treatment and limb lengthening procedures and can fail when pin loosening occurs. The resulting reduced stability can lead to delayed unions or even to non-unions, as well as to higher risk of infection [10].

0957–4530

The aim of this research was to evaluate bone remodelling at the interface with HA coated and uncoated pins in order to study the effects of HA coatings on the surrounding tissues and to define if it improves pin fixation.

Microstructural analysis of perimplant bone was performed using microbeam XRD. This technique together with histological, morphometric and microhardness evaluations, gives a better definition of the newly formed bone "quality", meaning bone mineralization and maturity.

Moreover, the aspects of coating degradation or structural transformation, as well as the wear phenomena, were examined by means of Chesley microcamera and conventional XRD.

2. Materials and methods

2.1. Implant materials and surgical procedure

Bicylindrical stainless steel external fixation commercially produced pins (Citieffe, Bologna, Italy) were used. The outer thread pin diameters were 4 and 5 mm. Pins were divided in two groups: one group of pins were plasma sprayed with HA (Biocoating, Flametal, Fornovo Taro, Pr 43045, Italy) to obtain a coating with a thickness ranging from 30 to 60 μm, and the other pins remained uncoated. The crystallinity ratio of hydroxyapatite, calculated by Roentgen ray spectroscopy, was $>70\%$, and the purity was $>97\%$ by mass spectroscopy. The hydroxyapatite powder contained traces of heavy elements below the limits set by the American Standard for Testing and Materials F1185-88 standard test. The Ca/P ratio was 1.67 ± 0.01.

Using the predrilling and tapping insertion technique, six pins of the same type were implanted monolaterally into the tibiae of mature sheep, and a monolateral fixator was assembled on the pins.

Three sheep received coated pins, and two received uncoated pins. The pins were numbered in proximal–distal order. The medial tibial mid-diaphysis was then exposed, between pins No 3 and 4, and a transverse 5 mm gap osteotomy was performed in order to stress the bone pin interface highly and to obtain unstable fixation of the fracture. The sheep were allowed normal activity. Six weeks after surgery sheep were euthanized. Pins 2–5 were not included in the present study and were used for other analyses, while pins 1 and 6 from each animal were processed for XRD analysis, after removal of the pin [11, 12]; uncoated pin 1 of one sheep was not examined.

2.2. Histological procedure

Bone segments about 2 cm thick were isolated and fixed in 20 ml of a 10% formalin solution buffered at pH 7.2. The samples were then dehydrated by warm methyl alcohol under vacuum, and methyl-methacrylate embedded.

The specimens were then transversally cut at the implant level by means of a diamond saw microtome model 1600 Leitz until the thickness of the slices was about 100 μm. On these sections a study was carried out and newly formed bone tissue in close contact with implants was analysed. As a control, bone tissue located at 1 mm from the implants was used.

2.3. XRD analysis

XRD analysis was performed with the microbeam XRD technique using a Chesley X-ray camera [13] that allowed the identification of the reflections ($h\,k\,l$) of the crystalline phase of the bone apatite. In this technique the X-ray beam is collimated so that the section of the beam at the specimen level is 50–100 μm in diameter. By placing a film perpendicularly to the incident beam, diffraction orders of the specimen are recorded onto the film and represented by different rings or reflections with a well defined radius, which characterize a particular substance. Crystallographic characterization on $0.002\,mm^2$ areas previously selected by microscopic examination can be obtained [14]. The crystallographic diffraction data of the bone tissue was compared with the crystallographic identification file of HA published by the Joint Committee on Powder Diffraction Standards (JCPDS File 9-432) [15]. The tests were performed using a Philips PW/1729 X-ray generator, producing CuK_α radiation, and by applying the following instrumental parameters: 25 kV, 25 mA, 100 μm diameter collimator, nickel filter, film–sample distance of 15 mm and 11 h exposure; the patterns were recorded on Kodak AA high-resolution films.

Five micro-areas were examined on each sample. The reflections recorded onto films can be converted, by microdensitometric radial scanning, into a graph that defines the 2θ angles, in degrees, which permits the calculation of the interplanar distance of each set of planes in the apatite lattice.

Ten radial scannings were performed for each film. These were used in order to define the crystallographic phases present and to determine the lattice parameters a and c as well as the lattice volume of the bone apatite crystallographic cell and to detect their modifications after contact with the implant.

The linear regression method was applied using two ($h\,k\,0$) reflections and three ($h\,k\,l$) reflections, i.e. (1 1 0), (2 1 0), (1 1 1), (2 1 2) and (2 2 1), according to the hydroxyapatite hexagonal structure. The following equations were used to assign hexagonal indices

$$d^2_{hk0} = 3/4(a^2/h^2 + hk + hl)$$

This can be used to determine the value of a. After a is known, the entire equation

$$d^2_{hkl} = \frac{1}{[4(h^2 + hk + k^2)/3a^2] + l^2/c^2}$$

can be used to determine the value of c [16].

The bone tissue found at a distance of 1 mm from the implant was used to obtain reference values for each group of animals. This provides a true control value as lattice parameters of the bone apatite phase are affected intensely by the type of tissue (cortical and

trabecular), the age of the animal and the histological treatment of the bone [17].

Crystalline particles of doubtful interpretation released into periprosthetic tissues from the HA coating were analysed and identified by microbeam XRD.

In order to assess the structural stability of HA coatings, coated pins after retrieval were examined using conventional powder diffraction analysis; XRD was carried out using a Philips powder Bragg–Brentano goniometer with a PW/1840 X-ray generator, producing CuK_α radiation, and by applying the following instrumental parameters: 40 kV, 40 mA, nickel filter and 9 h exposure and 5–70° 2θ with a 0.01° 2θ angular step-size. For comparison, the HA coating of two unimplanted pins was analysed.

Coating XRD patterns were fitted and matched with the crystallographic identification file of HA published by the JCPDS (File 9-432).

Profile fitting was performed using a Philips profile fitting program, which employed a Marquardt non-linear least squares algorithm. The program can identify no more than eight reflections. The profile fitting stops when convergence has been reached [18].

2.4. Calculations and statistical analysis

Data concerning bone apatite lattice parameters were expressed as arithmetic means plus and minus the standard deviations of the means ($m \pm$ SD) of the values obtained from five diffraction patterns for each pin.

The results were statistically evaluated by applying the student's t-test and using the StatView 4.5 software for Macintosh (Abacus Concepts). For each parameter, all values found for uncoated pins were compared: bone far from the implant versus bone at the interface. The same was made for the coated pin group. The software calculates the p values considered as statistically significant in comparison to bone apatite reference values. In all analyses $p < 0.05$ was considered as statistically significant.

3. Results

3.1. Bone

When studying the retrieved HA coated pins, XRD of the newly-formed bone close to the implant showed a ring pattern consistent with a polycrystalline structure A on (Fig. 1b); it confirmed histomorphometric data, reported in a previous study [11], that demonstrated a good interface between the bone and the HA coated pins (Fig. 1).

The recorded reflections expressed the d-values of a mineral with an apatitic-like phase and matched those of the JCPDS for HA (File 9-432).

Diffractograms were different depending on the mineralization level of the examined XRD-micro-areas: they showed especially hydroxyapatite reflections that were well resolved. By comparison, the amorphous component was not as evident; the mineral component appeared to be absent in some micro-areas. Moreover, it was noted that the (0 0 2) reflection of apatite crystallites showed a partial meridional orientation. Such orientation indicates the presence of longer crystallites regularly orientated along the c-axis, parallel to collagen fibres [19]. The diffractometric pattern found in the newly-formed tissue was therefore similar to that observed for the pre-existing bone (Fig. 1c). Lattice parameters of the apatite phase at the interface and far from the implant did not show statistically significant differences and the crystallographic cell was considered to be unaltered.

In uncoated implants XRD of the trabeculae maintaining a direct contact with the implant showed a normal apatitic structure (Fig. 2b). The orientation

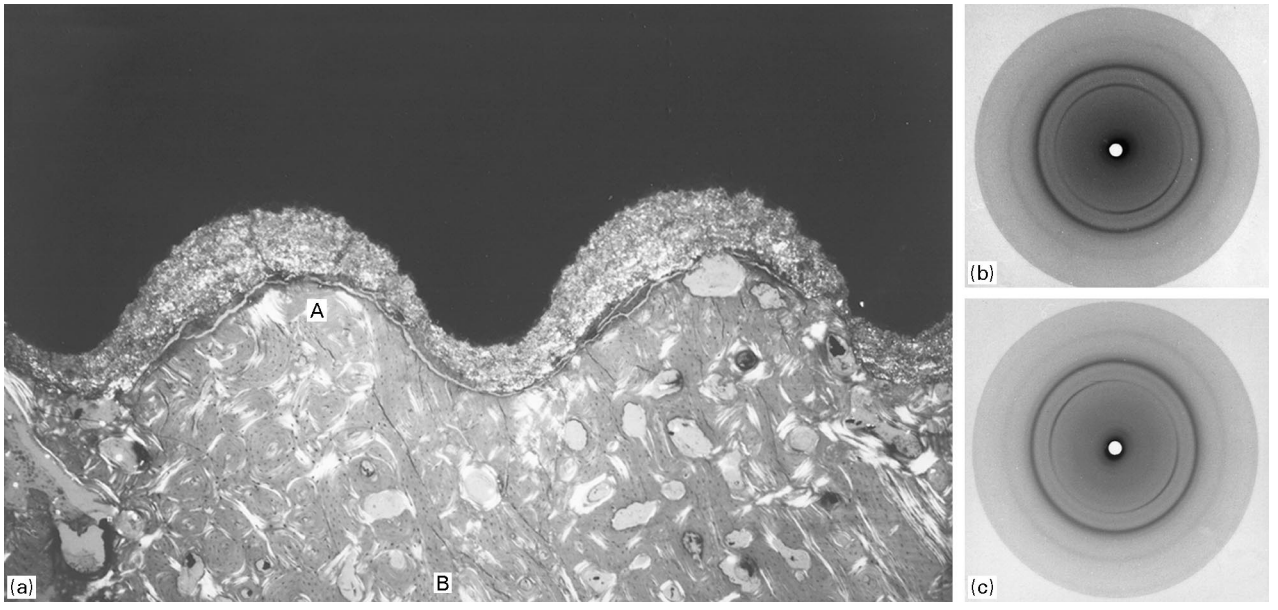

Figure 1 (a) Transverse section of a tibia at the level of a HA coated pin, retrieved six weeks after surgery. Good interface between the bone and the pin is clearly shown (trichromic stain, original magnification ×6.3). The XRD pattern of (b) the bone tissue at the interface with pin shows a normal apatitic structure (A), as does (c) the XRD pattern of the bone tissue far from the implant (B). The orientation effects of the (0 0 2) reflection are evident (Chesley microcamera, 25 kV, 25 mA, 11 h exposure).

Figure 2 (a) Transverse section of a tibia at the level of an uncoated pin. Not much contact between bone and implant was observed (trichromic stain, original magnification × 6.3). XRD of (b) the bone tissue maintaining a direct contact with the implant (A) shows a normal apatitic structure, but the bone is poorly mineralized, with an evident amorphous phase and low intensity apatite reflections. (Chesley microcamera, 25 kV, 25 mA, 11 h exposure). In contrast, bone tissue (c) far from the implant is normally mineralized (B).

effects of the (0 0 2) reflection were evident. Nevertheless, XRD showed an increase of poorly mineralized bone micro-areas with poor HA reflections and an evident amorphous phase fitting histological result that showed, after six weeks from implantation, a statistically significant decrease of bone–implant contact percentage occurring in uncoated pins with respect to coated ones (Fig. 2).

As the bone far from the pin was considered to be the true "control" for the interfacial bone, the lattice parameters of bone apatite at the interface were found to be statistically different from those recorded in the bone far from the pin in the uncoated pin group, although not different from the JCPDS values.

Fig. 3 shows a microdensitograph of an XRD pattern of the bone apatite recorded at the interface with a coated pin. The reflections 1 1 0, 1 1 1, 2 1 0, 2 1 2 and 2 2 1 were used in the lattice parameter and cell volume analyses.

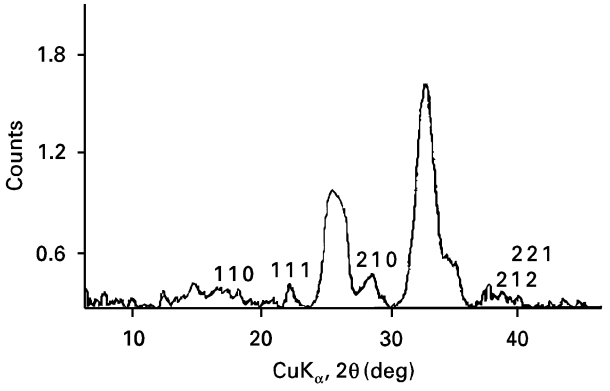

Figure 3 XRD pattern microdensitograph shows reflections used in lattice parameter analysis (1 1 0, 1 1 1, 2 1 0, 2 1 2, 2 2 1). (Chesley microcamera of the bone apatite at the interface with a coated pin, 25 kV, 25 mA, 11 h exposure, Ital Structures microdensitometer).

Table I shows the bone lattice parameters (*a* and *c* axis) and the cell volume, of perimplant bone in coated and uncoated implants; the results are expressed as the arithmetic mean ± the standard deviation of five determinations performed on each animal (both pins 1 and 6, except uncoated pin 1 of one sheep).

Table II shows the cumulative arithmetic mean ± the standard deviation of the results for each lattice parameter at the interface with the implant and, for comparison, far from it, respectively, in coated (30 determinations) and uncoated implants (15 determinations).

3.2. HA coating

The HA coating of implanted pins appeared histologically less compact after six weeks if compared with the coating of unimplanted ones; nevertheless, XRD pattern fit profiles, performed as described in Section 2.3, showed the main reflections of HA according to the JCPDS for HA (File 9-432) (Fig. 4).

In some cases also a partial disintegration of the coating occurred and some ceramic particles were found in the newly formed bone (Fig. 5). However, these particles seemed not to affect regular bone tissue mineralization; the XRD pattern and apatite lattice parameters of bone surrounding particles did not show significant differences in respect to the host bone.

4. Discussion

Calcium phosphate ceramics have the ability to act as osteoconductive materials. Numerous studies have demonstrated that ceramic coatings improve the attachment to surgical implants. Bone at the interface with implants is usually analysed with histological

TABLE I Bone lattice parameters, *a*-axis, *c*-axis and cell volume, of perimplant bone in coated and uncoated pins. Results are expressed as arithmetic mean ± standard deviation of five determinations performed on each sample

	Sample No.	Bone tissue far from the implant	Bone tissue close to the implant
Coated pins			
a-axis			
1	(animal no. I)	9.43 ± 0.09	9.45 ± 0.09
2	(animal no. I)	9.43 ± 0.06	9.42 ± 0.05
3	(animal no. II)	9.46 ± 0.09	9.44 ± 0.08
4	(animal no. II)	9.47 ± 0.09	9.41 ± 0.06
5	(animal no. III)	9.46 ± 0.10	9.45 ± 0.06
6	(animal no. III)	9.39 ± 0.05	9.39 ± 0.03
c-axis			
1	(animal no. I)	6.81 ± 0.16	6.74 ± 0.26
2	(animal no. I)	6.85 ± 0.33	6.80 ± 0.19
3	(animal no. II)	6.75 ± 0.16	6.71 ± 0.15
4	(animal no. II)	6.83 ± 0.13	6.81 ± 0.18
5	(animal no. III)	6.79 ± 0.27	6.83 ± 0.19
6	(animal no. III)	6.85 ± 0.16	6.89 ± 0.15
Cell volume			
1	(animal no. I)	517.82 ± 16.58	523.84 ± 17.90
2	(animal no. I)	524.96 ± 9.59	523.18 ± 21.10
3	(animal no. II)	523.98 ± 21.72	523.22 ± 18.27
4	(animal no. II)	527.18 ± 14.04	522.65 ± 13.33
5	(animal no. III)	527.66 ± 22.90	525.17 ± 19.99
6	(animal no. III)	527.94 ± 21.39	525.88 ± 13.99
Uncoated pins			
a-axis			
1	(animal no. I)	9.38 ± 0.39	9.41 ± 0.07
2	(animal no. I)	9.36 ± 0.01	9.40 ± 0.05
3	(animal no. II)	9.41 ± 0.04	9.42 ± 0.06
4	(animal no. II)	Unsuitable sample	Unsuitable sample
c-axis			
1	(animal no. I)	6.84 ± 0.13	6.79 ± 0.16
2	(animal no. I)	6.93 ± 0.21	6.79 ± 0.15
3	(animal no. II)	6.79 ± 0.13	6.81 ± 0.26
4	(animal no. II)	Unsuitable sample	Unsuitable sample
Cell volume			
1	(animal no. I)	524.23 ± 10.25	519.82 ± 12.90
2	(animal no. I)	529.75 ± 14.34	521.46 ± 10.79
3	(animal no. II)	521.39 ± 9.06	524.01 ± 18.51
4	(animal no. II)	Unsuitable sample	Unsuitable sample

TABLE II The table shows the arithmetic mean ± standard deviation of 30 and 15 determinations, respectively, in coated and uncoated implants, for each lattice parameter at the interface with the implant and, for comparison, far from it. No statistically significant (n.s.) variation between newly formed and host bone is observed in coated implants, whereas a significant variation is observed in uncoated ones

Apatite lattice parameters	Bone tissue far from the implant	Bone tissue close to the implant	*p*
Coated pins			
a-axis	9.44 ± 0.08	9.43 ± 0.07	n.s.
c-axis	6.81 ± 0.24	6.80 ± 0.19	n.s.
Cell volume	525.50 ± 19.30	523.70 ± 18.60	n.s.
Uncoated pins			
a-axis	9.38 ± 0.04	9.41 ± 0.07	0.005
c-axis	6.85 ± 0.17	6.79 ± 0.18	0.007
Cell volume	524.90 ± 11.60	521.50 ± 13.80	0.020

methods and microstructural analyses, but XRD has rarely been applied to its analysis.

A conventional XRD technique has been used by various investigators [10, 11] to quantify the crystallinity of the bone tissue mineral phase. However, such a procedure can be used only with large-size samples, and does not distinguish newly-formed bone from the pre-existing host tissue. By contrast, an XRD technique with sample microfocusing permits identification of the mineral component of the bone trabeculae on micro-areas selected under light microscopy and yields information on the texture of the apatite crystallites and on their orientation induced by collagen fibres and mechanical loads.

In this research XRD was used to examine the mineral phase of bone at the interface with coated and

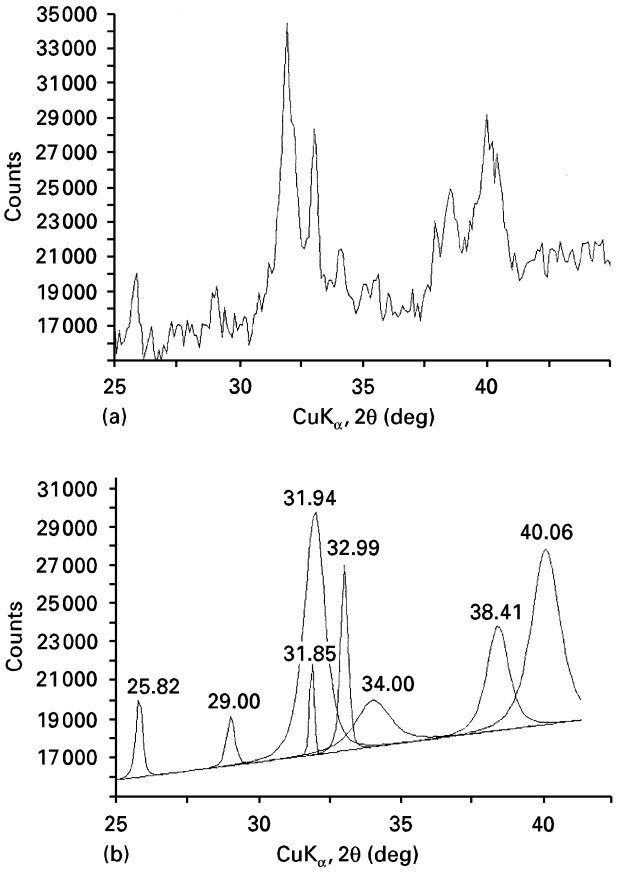

Figure 4 (a) XRD pattern of a HA coating retrieved six months after implant (40 kV, 40 mA, 9 h exposure), and (b) the fit profile of the XRD pattern shows eight main HA reflections.

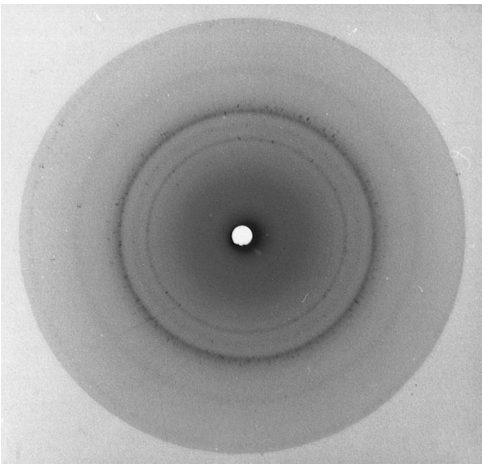

Figure 5 XRD pattern of a HA particle released in the perimplant bone (Chesley microcamera, 25 kV, 25 mA, 11 h exposure).

uncoated pins in order to evaluate the microstructural interactions between the surface of the metal or HA coating and apatite crystals. Particularly, using the diffractometric technique we evaluated whether ions released due to implant wear or corrosion had induced changes in the lattice parameters that were strongly influenced by possible ion substitutions occurring in the bone apatite.

It has been demonstrated that the mineralization process is strongly influenced by ionic diffusion during crystal nuclei formation and growth, after amorphous calcium phosphate accretion to collagen fibres. Substitution of ions in the apatite structure can result in an expansion of lattice parameters along the *a*- and *c*-axes of the crystal [20]; for example, Mo toxicity can be related to substitution for phosphate, subverting the role of the latter in the initiating steps of osteogenesis as well as a constituent of the crystal lattice of bone apatite [21].

This experimental technique is not reliable enough to obtain very useful or accurate lattice parameters; the technique does, however, offer a guide to the change in the crystalline–amorphous nature of new bone at the interface.

Microstructural characterization of the bone at the interface with the pins showed that HA coating improves the degree of mineralization at the interface, whereas an increase in the amorphous phase of the bone tissue in uncoated pins has occurred. Moreover, bony apatite is not modified during implant in coated pins, the cell parameters of this bone are not altered in respect to normal bone, showing that HA does not interfere with the mineralization process. Our results fit with previous studies [22, 23].

By comparison, bony apatite in the uncoated pin experiments showed a significant change of apatite lattice parameters; it has been hypothesized that the presence of metal particles released in periprosthetic tissues could alter the mineralization process, causing a change in the apatite lattice parameters probably due to a change in the composition of the apatite phase.

5. Conclusions

It can be concluded that, six weeks after surgery, perimplant bone tissue does not reach complete maturity in coated and uncoated pins, but HA coating improves the mineralization process and the "quality" of the newly formed bone at the interface. HA coating fragments, rarely released in perimplant bone, do not interfere with bone mineralization. This was achieved by XRD and by recording the lattice parameters in the bone around the fragments (data not shown).

These observations fit histomorphometric results in the same cases [11]. The analysis of the histological specimens demonstrate that the bone tissue close to HA-coated implants is often in direct contact with the implant surface without the presence of an intervening fibrous tissue layer. On the contrary, bone tissue near uncoated pins does not always show a direct contact with the metal that could lead to a weakening of the fixation of the prosthesis.

HA pin coating is likely to improve the performance of external fixators, by favouring bone apposition and reducing failures due to pin loosening.

Acknowledgements

This research was partially supported by grants from Istituti Ortopedici Rizzoli, Ricerca Corrente and partially by grants of Murst 40%.

References

1. H. W. DENISSEN, *Ultramicrosc.* **5** (1980) 124.
2. M. JARCHO, *Clin. Orthop. Rel. Res.* **157** (1981) 259.
3. B. M. TRACY and R. H. DOREMUS, *J. Biomed. Mater. Res.* **18** (1984) 719.
4. H. W. DENISSEN, W. WALK, A. A. H. VELDHUIS and A. VAN DER HOOFF, *J. Prosthet. Dent.* **61** (1989) 706.
5. R. G. T. GEESINK, *Clin. Orthop.* **261** (1990) 539.
6. B. C. WANG, E. CHANG, C. Y. YANG and D. TU, *J. Mater. Sci. Mater. Med.* **4** (1993) 394.
7. K. THOMAS, J. F. KAY, S. D. COOK and M. JARCHO, *J. Biomed. Mater. Res.* **21** (1987) 1395.
8. K. A. PETTINE, E. Y. CHAO and P. KELLY, *Clin. Orthop.* **293** (1993) 18.
9. A. MORONI, V. CAJA, S. STEA and M. VISENTIN, in "Bioceramics", Vol. VI, edited by P. Ducheyne and D. Christiansen (Butterworth-Heinemann, Oxford, 1993) pp. 239–44.
10. J. ORLY, M. GREGOIRE, J. MENANTEAU, M. HEUGHEBAERT and B. KEREBEL, *Calcif. Tissue Int.* **45** (1989) 20.
11. S. STEA, M. VISENTIN, L. SAVARINO, M. E. DONATI, A. MORONI, V. CAJA and A. PIZZOFERRATO, *J. Mater. Sci. Mater. Med.* **6** (1995) 455.
12. S. STEA, M. VISENTIN, L. SAVARINO, G. CIAPETTI, M. E. DONATI, A. MORONI, V. CAJA and A. PIZZOFERRATO, *J. Biomed. Mater. Res.* **29** (1995) 695.
13. CHESLEY, *Rev. Sci. Instr.* **18** (1947) 422.
14. L. SAVARINO, E. CENNI, S. STEA, M. E. DONATI, G. PAGANETTO, A. MORONI, A. TONI and A. PIZZOFERRATO, *Biomaterials* **14** (1993) 900.
15. Joint Committee on Powder Diffraction Standard, File 9-432 (1938).
16. L. V. AZÀROFF and M. J. BUERGER, in "The powder method in X-ray crystallography" (McGraw-Hill, New York, 1958) pp. 82–3.
17. R. G. HANDSCHIN and W. B. STERN, *Calcif. Tissue Int.* **51** (1992) 111.
18. W. N. SCHREINER and R. JENKINS, *Adv. X-ray Anal.* **26** (1983) 141.
19. S. A. JACKSON, A. G. CARTWRIGHT and D. LEWIS, *Calcif. Tissue Res.* **25** (1972) 217.
20. R. Z. LEGEROS, L. SINGER, R. H. OPHAUG, G. QUIROLGICO, A. THEIN and J. P. LEGEROS, in "Osteoporosis" (J. Menczel, M. Makin and R. Steinberg, Eds), J. Wiley, 1982, pp. 327–341.
21. N. D. PRIEST and F. L. VAN DE VYVER, in "Trace metals and fluoride in bones and teeth", (CRC Press, Boca Raton, Boston, 1990) p. 238.
22. W. J. A. DHERT, KLEI CPAJ, J. A. JANSEN, E. A. VAN DER VELD, R. C. VRIESDE, M. ROZING and K. DE GROOT, *J. Biomed. Mater. Res.* **27** (1993) 127.
23. J. A. JANSEN, J. P. C. M. VAN DER WAERDEN and J. G. G. WOLKE, *ibid.* **27** (1993) 603.

Received 15 March 1996
and accepted 1 September 1997